Preprints (www.preprints.org) | NOT PEER-REVIEWED | Posted: 23 January 2017 doi:10.20944/preprints201701.0099.v1

CO_2 Gasification Reactivity of Chars Derived From Zhundong Coal

Yun Liu, Yanjun Guan, Kai Zhang *

Beijing Key Laboratory of Emission Surveillance and Control for Thermal Power Generation, North China Electric Power University, Beijing 102206, China; liuyun.1988.2008@163.com (Y.L.); gyj0627@gmail.com(Y.G.)

* Correspondence: kzhang@ncepu.edu.cn; Tel.: +86-10-6177-2413

Abstract: Coal gasification with carbon dioxide is a process for generating clean gaseous fuels and relieving greenhouse effect. Zhundong coal has high alkali and alkali earth metals (AAEMs) content, medium volatile and low ash in nature. Isothermal CO_2 gasification of char derived from Zhundong coal (R-char) and char from acid washing R-char (AR-char) are performed in thermo-gravimetric analyzer (TGA). The effect of AAEMs is investigated on the gasification behavior in the range of temperatures 1073 K to 1273 K. The carbon conversion increases rapidly with increasing reaction temperature and CO_2 concentration. R-char has high gasification rate and carbon conversion compared with AR-char. The accuracy of the free-model approach for calculating activation energy at different conversions is validated by compared with different kinetic models (volume reaction model, distributed activation energy model). Moreover, R-char gasification with CO_2 shows a compensation effect as the Arrhenius parameters (E_A and k_0) increase or decrease simultaneously.

Keywords: Zhundong coal; char; CO_2 gasification; alkali and alkaline earth metals

1. Introduction

The greenhouse effect primarily due to CO_2 emissions, which has become one of important issues in related to energy, environment and economy [1]. The statistics indicated the combustion of fossil fuels was the primary anthropogenic cause of CO_2 emissions [2]. Therefore, it is urgent to develop low-carbon approaches for clean coal utilization. Gasification is generally considered as an efficient process for coal conversion, especially, CO_2 gasification has been regarded as a potential technology to directly utilize greenhouse gas [3]. However, the gasification reaction with CO_2 is relatively slow by compared with other gasification agents (i.e. O_2, H_2O). Previous investigators have concluded that high reactive coals are particularly suitable for CO_2 gasification [3-5]. Zhundong coal, with an estimated reserve of 3.9 Gt, is a super large energy source in China [6]. It has high reactivity, medium volatile and low ash. Furthermore, it has high alkali and alkali earth metals (AAEMs) which play a significant role on gasification process [7-9].

The catalytic effect of AAEMs on the reactivity of CO_2 gasification has been investigated [10-13]. Li and co-workers [10,11] explored the volatilization and catalytic effects of AAEMs on the pyrolysis and gasification of Victorian brown coal. They concluded that NaCl in the brown coal was mainly released as Na and Cl separately rather than as NaCl molecules, and the volatile-char interactions were affected by the valence of the AAEMs in the char. Ding et al. [12] considered the catalytic ability and concentration of AAEMs were positively correlated below a certain concentration. Walk et al. [13] identified that catalytic ability of AAEMs on

Preprints (www.preprints.org) | NOT PEER-REVIEWED | Posted: 23 January 2017 doi:10.20944/preprints201701.0099.v1

CO_2 gasification decreased in the order of Na > K > Ca from anthracite to lignite, and pointed the catalytic ability was dependent on the concentration, chemical forms, and dispersion of AAEMs in coal. Meanwhile, several other studies focused on the transformation of Na, Cl and silica [10,14-16]. Kosminski et al. [15,16] examined the transformation of Na during the gasification of South Australian lignite. Their results indicated that release of Na and Cl was disproportionate to NaCl in coal. Kosminski et al. [17] also investigated the reaction between Na and silica or kaolin, and found liquid sodium silicates were major reaction products of Na and silica.

It is necessary to understand the reaction kinetics under controlled laboratory conditions to support large scale gasification trials, which makes the process may easily be modelled from the desired reaction conditions when the fundamental parameters are obtained. As for CO_2 gasification of coal, the high char reactivity was essential for achieving high conversion levels as the gasification rate was limiting step in comparison to devolatilization of coal [5,18]. What is more, the kinetic modeling of char was crucial in determining the rate of whole coal gasification [3]. The common kinetic models, such as volumetric reaction model (VRM) [19] and distributed activation energy model (DAEM) [20], have been proposed to widely predict reaction of coal gasification [21,22]. Activation energy (E_A) is an important parameter to evaluate reaction in kinetic analysis. A new method, free-model approach (FMA) as an alternative approach can estimate E_A without assuming a kinetic model [23]. However, the E_A obtained from the free-model approach maybe lead to some unexpected results for CO_2 gasification.

The objective of this study is to determine the CO_2 gasification performance of chars derived from Zhundong coal, by considering the effect of reaction temperature and residence time, CO_2 concentration and AAMEs content. Two kinetic models, i.e., VRM and DAEM, are used to investigate the gasification reactivity of char. The prediction ability of activation energy for the free-model approach is evaluated by comparing with the above two kinetic model during CO_2 gasification. In addition, the relation of E_A and k_0 is explored during char gasification.

2. Materials and methods

2.1. Char preparation

Coal used in this study is from the east of the Junggar Basin in Xinjiang, China. Before experiments, all samples are dried in vacuum oven at 378 K for 2 h. To eliminate the effect of intra pore diffusion on the gasification rate, coal samples are ground and sieved with particle size less than 90 μm [19,24]. The proximate and ultimate analyses of Zhundong coal are listed in Table 1.

The chars are obtained by devolatilized the coal samples in the tubular reactor at the temperature 1073 K, which is equipped with the intake part, sampling part and temperature control part. A detailed description of the test unit is shown in Figure 1. Before experiments, a sweep N_2 gas flow of 400 mL/min was used to remove the air in the device for 30 min. Then, the device is heated at a rate of 10 K/min. Once the temperature is reached 1073 K, coal samples are loaded into the reactor rapidly. Then the samples are maintained for 30 min at the temperature under a continuous nitrogen atmosphere, and then the samples are pushed to the cooling zone promptly by sample push rod. After cooling to room temperature, the char

Preprints (www.preprints.org) | NOT PEER-REVIEWED | Posted: 23 January 2017 doi:10.20944/preprints201701.0099.v1

sample named as R-char is taken out, a part of which is stored in a desiccator, whilst the other is stirred in 0.1 mol/L sulphuric acid for about 24 h under nitrogen atmosphere before washing with distilled water. After drying this kind of char is referred to as AR-char, which is also stored in the desiccator. Prior to testing, all the char samples are dried at 378 K for more than 24 h.

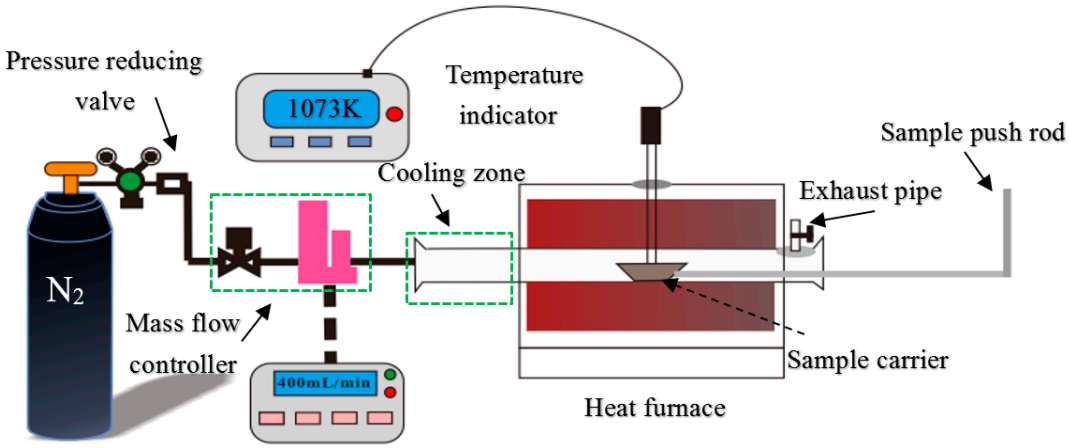

Figure 1. Schematic diagram of the tubular reactor

The composition of ash is determined by X-ray fluorescence (Shimadzu XRF-1800). According to AS 1038.14.1-2003 (R2013), low temperature ash of R-char and AR-char samples are prepared in a muffle furnace at 773 K. The primary compositions of ash are listed in Table 2. It is clear that the ash from R-char is dominated by basic oxides (CaO, MgO, Na_2O, Fe_2O_3, and K_2O) with a minor fraction of acidic oxides (SiO_2, Al_2O_3 and TiO_2). Thus, it can be obtained the data of 3.15 by the ratio of basic oxides to acid oxides. In contrast, the AR-char ash has a low B/A ratio approximately 0.15, containing high acidic oxides including SiO_2 and Al_2O.

In addition, A scanning electron microscopy (Tescan Vega 3) coupled with energy dispersive X-ray spectroscopy are used to observe the morphology of the samples, and to obtain semi-quantitative elemental analysis of the char particles.

Table 1. Proximate and ultimate analysis of Zhundong coal

Proximate analysis (wt.%, air dry)				Ultimate analysis (wt.%, dry)				
V	FC	A	M	C	H	O[a]	N	S
28.15	59.25	3.08	9.52	70.79	3.86	24.26	0.56	0.53

[a] Oxygen was measured By subtraction

Table 2. Ash analysis of the char samples ashed at 773 K

Samples (wt. %)	CaO	MgO	Na_2O	K_2O	Fe_2O_3	SiO_2	TiO_2	Al_2O_3	B/A ratio
R-char	37.85	8.62	6.18	0.55	4.06	10.39	0.37	7.42	3.15
AR-char	7.34	1.15	0.61	0.68	1.71	48.98	0.92	27.54	0.15

2.2. Gasification procedure experiments

Gasification tests are carried out in the thermo-gravimetric analyzer (NETZSCH STA 449F3). All char samples are gasified isothermally at four different temperatures from 1073 K to 1223 K under a continuous nitrogen flow of 80 mL/min. Figure 2 shows the effect of CO_2

Preprints (www.preprints.org) | NOT PEER-REVIEWED | Posted: 23 January 2017 doi:10.20944/preprints201701.0099.v1

flows on R-char gasification. Experimental results indicate that the carbon conversion increases significantly with an increase in CO_2 flow when it is less than 60 mL/min, whilst the conversion hardly changes when the flow is more than 60 mL/min. Combined with former, particles less than 90 μm can ignore intra pore diffusion, and flow of 80 mL/min can eliminate external diffusion. In all cases the experimental results represent average values of at least three duplicate runs.

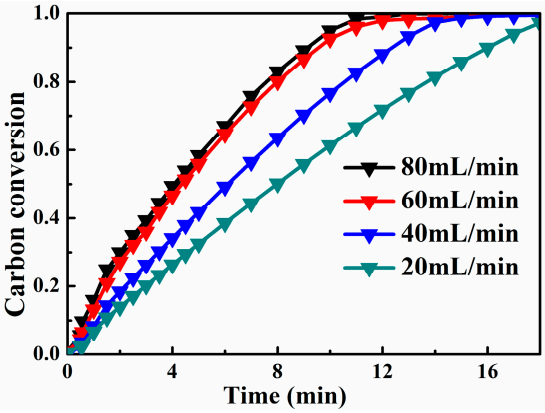

Figure 2. Comparison of conversions and times for R-char at different CO_2 flows

In this study, carbon conversion rate for gasification, x, is:

$$x = \frac{m_0 - m_t}{m_0 - m_{ash}} \quad (1)$$

where m_0 is the initial mass of the sample, m_t is the mass at a particular time, and m_{ash} is the mass of the ash.

Gasification rate is defined as differential of carbon conversion to gasification time, the gasification rate, r, is expressed as:

$$r = \frac{dx}{dt} \quad (2)$$

where, x is the carbon conversion rate, t refers to time.

2.3. Kinetic models and free-model approach

There are many kinetic models for description of CO_2 gasification. Two common models [19,20] are adopted in this study.

The first model is volumetric reaction model (VRM), which is an ideal model for describing gas-solid reaction. The reaction is considered to take place everywhere in the volume of the particle, as below:

$$\frac{dX_c}{dt} = k_{VRM}(1 - X_c) \Rightarrow X_c = 1 - \exp(-k_{VRM}) \Rightarrow \ln(1 - X_c) = k_{VRM} \quad (3)$$

where, k_{VRM} is the rate coefficient, t is time, Xc is the carbon conversion rate.

The second model is distributed activation energy model (DAEM). This model assumes that the char gasification reaction consists of many parallel first order reactions, and integrated activation energy of char gasification presents distribution function [20]. Under the condition of isothermal DAEM is given by:

$$lnt = -\ln k_0 + ln[-ln(1 - X)] + \frac{E}{R} \cdot \frac{1}{T} \quad (4)$$

Preprints (www.preprints.org) | NOT PEER-REVIEWED | Posted: 23 January 2017 doi:10.20944/preprints201701.0099.v1

where, X is the carbon conversion rate, E is activation energy, R is molar gas constant and k_0 refers to the pre-exponential factor, min^{-1}.

Making a curve (lnt~$1/T$) can get straight slope and intercept at the same conversion rate on isothermal gasification experiments, which can obtain average E and k_0 refer to carbon conversion rate in the process of gasification temperature range.

The free-model approach was recently proposed to obtain the activation energy when gasification temperature was below 1273 K [22,23]. The method can be used to obtain the parameters of the Arrhenius equation for a set of isothermal experiments, and it can apply to scaling industrial processes or testing the consistency of a particular kinetic mode [22]. The activation energy can be calculated by this method, based on a deduction from the Arrhenius equation and a general rate law, without transformation of variables or assumption of a particular kinetic model. The advantage of this method is required only one regression, rather than the n+1 (n is the number of isothermal experiments) when a kinetic model is used. The plot of the logarithm of residence time, ln (time), for a particular conversion versus the reciprocal of temperature, $1/T$, follows a linear trend in the same way.

3. Results and discussions

3.1 Effect of temperature on gasification

The processed conversion results for samples are presented in Figure 3. Comparison of conversions and times for AR-char and R-char are deliberated at different temperatures. The time scale has been truncated to better display the high temperature data. The conversion rates of both samples increase with increasing temperature from 1073 K to 1223 K. By increasing gasification temperature, R-char is quite reactive to yield high carbon conversions in reasonable time (51.59% at 1123 K/11 min), while almost complete conversion is achieved at high temperatures and prolonged reaction times (99.02% at 1173 K/18 min). It takes approximate 12 min to complete carbon conversion at higher gasification temperature (1233 K). Similarly, Skodras et al. [25] concluded that reaction time was significantly reduced with an increase in temperature and 10 min was considered adequate for complete conversion at 1123 K and 1173 K.

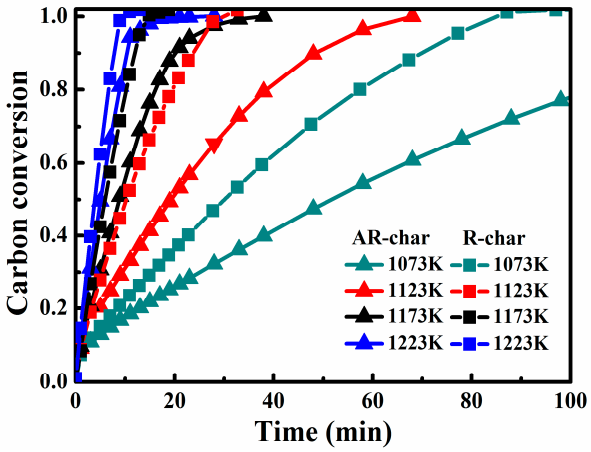

Figure 3. Comparison of conversions and times for AR-char and R-char at different temperatures

The reaction rate of R-char is faster than that of AR-char at the same time, especially at

Preprints (www.preprints.org) | NOT PEER-REVIEWED | Posted: 23 January 2017 doi:10.20944/preprints201701.0099.v1

low temperatures. This is largely due to the alkali and alkali earth metals play an important role in gasification at low temperature zone. The effect of alkali and alkali earth metals on gasification rate decreases with increasing reaction temperature.

According to molecular collision theory [25], changes in the number of reactive collisions are taking place during the reaction, and the amount of active sites is also alterant. The rate of reaction is proportional to the number of active sites. The more active sites are, the easier gasification reactions happen. It is well known that the amount of reactive collisions increases with temperature. Therefore, it can be obtained that carbon conversion rises at high temperatures.

3.2 Effect of CO_2 concentration

The effect of CO_2 concentration on the carbon conversion for AR-char and R-char gasification is examined at the temperature of 1173 K. As presented in Figure 4, the conversion rate increases with an increase of CO_2 concentration at their corresponding time. Furthermore, the reaction time of R-char (Figure 4a) and AR-char (Figure 4b) are significantly reduced with the concentration of gasification agent increasing from 25% v/v up to 75% v/v. When operated at the same condition, the conversion rate of R-char is higher than that of the AR-char in the whole range process. The reactivity of the R-char (Figure 4a) or AR-char (Figure 4b) has no substantial difference, as gasification with 25% v/v and 37% v/v of CO_2. Therefore, it has little effect on the carbon conversion at low concentration (below 37% v/v) under the same condition. Similar results were obtained for the CO_2 gasification of Argentinean subbituminous chars [26]. The gasification reactivity of R-char is higher than AR-char under the identical conditions, which is probably attributed to more alkali and alkaline earth metals in R-char than AR-char (in Table 2).

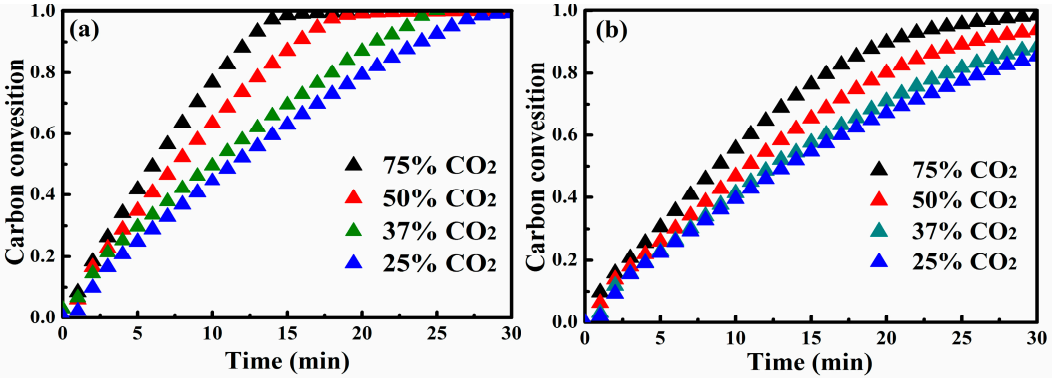

Figure 4. Comparison of conversions and times for R-char (**a**) and AR-char (**b**) at various CO_2 concentrations

3.3 Effect of AAEMs during gasification

R-char and AR-char are gasified with CO_2 in order to study the effect of alkali and alkali earth metals (AAEMs) on gasification rate. Gasification rate for the samples (R-char, AR-char) rises then reduces, as shown in Figure 5. It reaches the maximum when X (carbon conversion rate) is almost equal to 0.08, at various temperatures (1073 K, 1123 K, 1173 K, 1223 K). The increase in gasification rate is mainly because the active specific surface area is enlarged. However, the char activity decreases gradually along with the chemical reaction proceeding. The specific surface should be reduced due to pores broken and carbon particles consumed. It

Preprints (www.preprints.org) | NOT PEER-REVIEWED | Posted: 23 January 2017 doi:10.20944/preprints201701.0099.v1

is difficult to access to the active carbon, which results in gasification rate decreasing.

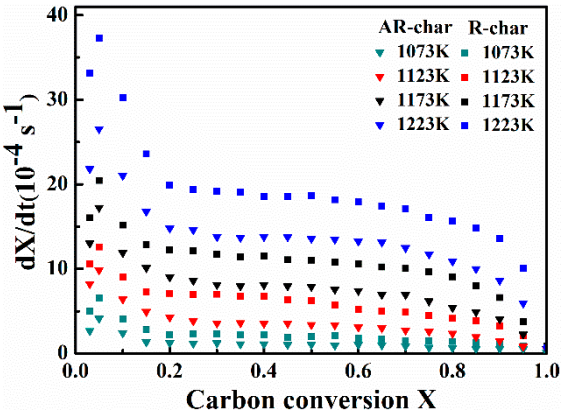

Figure 5. Comparison of gasification rates and conversions for R-char and AR-char at various temperatures

Figure 6 and Figure 7 show the SEM images of R-char and AR-char, and EDS results of elemental analysis (Ca, Mg, Na, Fe, K) at selected spots. Each element concentration is proportional to the corresponding color depth. It can be seen that element concentration of R-char is in the order Ca > Mg > Na > Fe > K. The concentration of five elements (Ca, Mg, Na, Fe, K) of R-char is much more than that of AR-char, which proves that acid can remove a lot of AAMEs in R-char. The results are consistent with the consequence of Table 2.

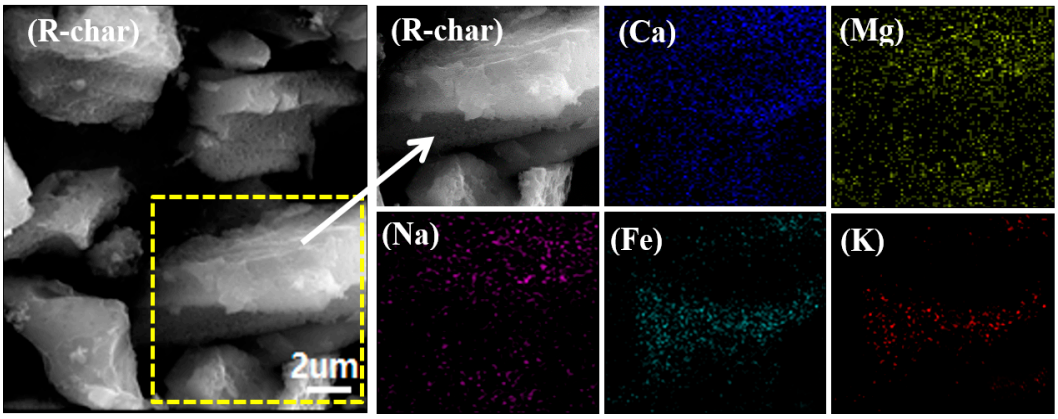

Figure 6. SEM morphology of R-char and EDS results of elemental analysis at selected spots

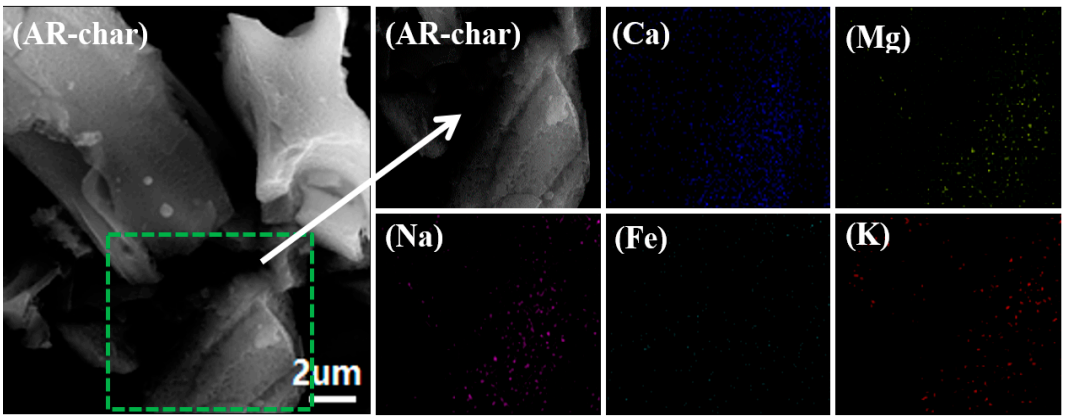

Figure 7. SEM morphology of AR-char and EDS results of elemental analysis at selected spots

Preprints (www.preprints.org) | NOT PEER-REVIEWED | Posted: 23 January 2017 doi:10.20944/preprints201701.0099.v1

It can be seen for the two chars that the gasification rate increases with increasing temperature. Furthermore, the reaction rate of R-char is higher than that of AR-char, especially at high temperatures (1173 K, 1223 K), except that the reaction rate for two chars is similar at the low temperature (1073 K) in Figure 5. Xiong et al. [4] conducted experiments of char gasification in a PTGA and concluded that alkali metal influences on reaction rate, which could reduce gasification activation energy and improve the gasification rate. As presented in Table 2, the B/A ratio of R-char is 3.15 in ash analysis, which is much higher than that of AR-char (0.15), and the basic oxides content of R-char is much higher in comparison to the AR-char except K. Figure 6 and Figure 7 also draw a similar conclusion that AAEMs contents are much higher in R-char. This implies that the basic oxides (AAEMs) have a catalytic role rather than acid oxides on the gasification. Yang et al. [27] have studied occurrence modes and contents of AAEMs in three kinds of Zhundong coals. It was found that Na was mainly water soluble (Na_w/Na_{total} = 50-85%), which was halite or in the form of surface bound Na^+. Ca and Mg were mainly acid soluble (Ca_{ac}/Ca_{total} = 60-90%, Mg_{ac}/Mg_{total} = 45-90%), which were carbonates with a little amount of sulfates. Moreover, the reaction rates of two samples are almost same at 1073 K, because temperature has significant influence on the rate of gasification rather than amount of AAEMs at low temperature. In our study, the content of K is slightly higher in ash of AR-char, since pickling hardly has effect on low K in char from Zhundong coal. However, other AAEM elements in the ash are decreasing obviously after acid pickling, which results in content of K relative increment.

3.4 Estimation of activation energy

As shown in Table 3, the coefficient of determination is higher than 0.98 for almost all cases. The activation energy calculated from free-model approach is close to that calculated from VRM and DAEM. This means that the free-model approach is feasible to calculate activation energy. Theoretically, activation energy should be constant and independent of the conversion. However, the activation energy calculated at lower conversion rate is smaller than at a higher conversion in this study. This may be attributed to part of the inactivated and lost AAEMs during the gasification [22,26]. In fact, if the reaction follows the same mechanism in the whole conversion range, the activation energy should be almost the same, which are calculated at different conversions.

Table 3. Activation energy (kJ/mol) at different conversion rates

Sample	R-char						AR-char					
	VRM		DEAM		FMA		VRM		DEAM		FMA	
	E_A	R^2	E_A	R^2	E_A	R^2	E_A	R^2	E_A	R^2	E_A	R^2
X=0.25	153.321	0.995	152.024	0.992	154.205	0.985	166.247	0.991	164.985	0.983	165.557	0.987
X=0.5	170.482	0.996	168.958	0.986	171.283	0.988	185.335	0.979	184.901	0.991	186.007	0.997
X=0.8	180.527	0.995	181.208	0.981	182.197	0.993	196.741	0.989	195.024	0.992	197.493	0.989

3.5 Compensation effect

The VRM is employed to calculate the E_A and k_0. As shown in Figure 8, the VRM gives a

Preprints (www.preprints.org) | NOT PEER-REVIEWED | Posted: 23 January 2017 doi:10.20944/preprints201701.0099.v1

better description about the conversion among the study temperature region. The model fits better at the lower temperatures (1073 K, 1123 K) than at the higher one (1223 K). This is consistent with the finding on non-catalytic steam gasification of lignite char [28].

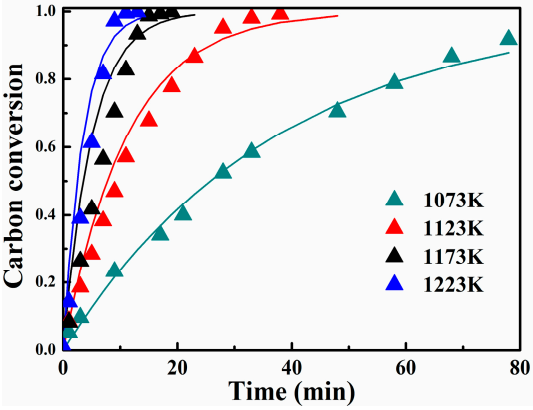

Figure 8. Comparison of conversions and times for R-char and calculated with VRM

The kinetic parameters of E_A and k_0 are showed in Table 4. The Arrhenius parameters (E_A, k_0) increase or decrease simultaneously, exhibiting a compensation effect. The E_A increases firstly and decreases subsequently as gasification time prolonging. It takes place when it is broken for the stronger bonds of carbon atoms. Therefore, the chemical reaction should overcome a higher energy barrier, which results in increasing activation energy for gasification. The structure of coal char is fractured (shown in Figure 6 and Figure 7), when carbonaceous material has already been expended, and activation energy decreases at longer reaction time.

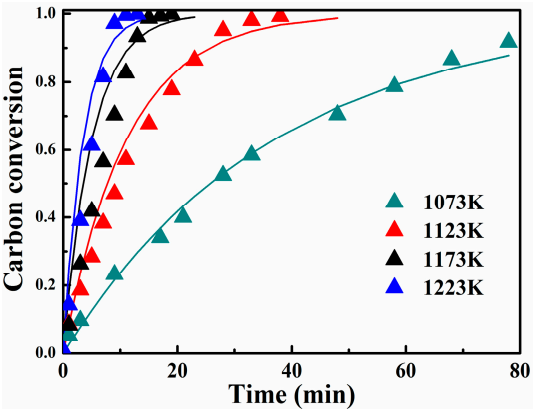

Figure 8. Comparison of conversions and times for R-char and calculated with VRM

Table 4. Activation energy, E_A, and pre-exponential factor, k_0, for isothermal CO_2 gasification

Time (min)	Activation energy, E_A, (kJ/mol)	Pre-exponential factor, k_0,(min^{-1})
1	100.30	4.85×10^{3}
5	180.37	1.79×10^{7}
10	244.70	1.82×10^{10}
15	266.94	7.68×10^{10}
20	227.53	2.78×10^{9}
25	189.48	1.93×10^{7}
30	120.52	1.40×10^{4}

Figure 9 illustrates the compensation effect in the study. A generalized interpretation

Preprints (www.preprints.org) | NOT PEER-REVIEWED | Posted: 23 January 2017 doi:10.20944/preprints201701.0099.v1

between k_0 and E_A describes a linear correlation [20]. Some rise of the E_A is accompanied with a simultaneous increase of k_0 among 10-15 min; while, some decrease of E_A is compensated by decrease of k_0 after 15 min. The two lines have a linear interrelationship with very good approximation (R^2 = 0.992 and 0.996).

Different carbon atoms of ground-state energy are gasified as the CO_2 gasification proceeding. Nevertheless, the number of active collisions is also increased. In order for chemical reaction to happen, it is necessary for the molecules to have correct orientation and sufficient energy to overcome the activation energy barrier [5]. However, not all collisions are in the correct orientation or full of energy in the chemical reaction. The E_A is the least value of energy for particular chemical reaction in gasification to take place. In the Arrhenius equation, k_0 is constant accounting for the crowd of rate-influencing parameters, such as molecular orientation, gaseous reactant concentration, active sites and so on.

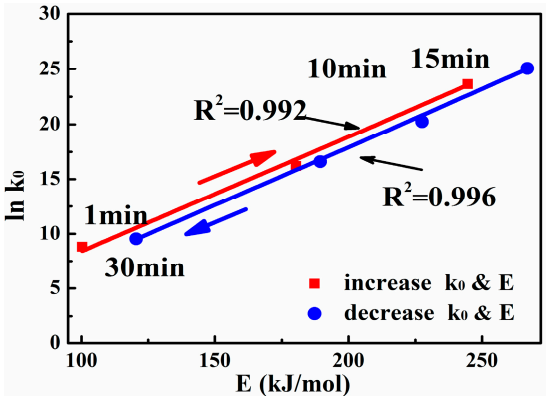

Figure 9. Compensation effect in isothermal CO_2 gasification of R-char

4. Conclusions

The CO_2 gasification reactivity of chars derived from Zhundong coal is determined by thermo-gravimetric analysis. The following conclusions are obtained from this work:

(1) Carbon conversion rate increases with increasing temperature and CO_2 concentration.

(2) The reactivity of AR-char is much lower than that of R-char, which identifies that alkali and alkali earth metals play a catalytic role in CO_2 gasification.

(3) Free-model approach is suitable for the calculation of activation energy by compared to volumetric reaction model and distributed activation energy model.

(4) Arrhenius parameters (E_A, k_0) increase or decrease simultaneously, exhibiting a compensation effect of the gasification process.

Acknowledgements: Authors gratefully acknowledge National Natural Science Foundation of China (91434120) and Major Special Project of Shanxi Province (MD2014-03, MD2015-01).

Author Contributions: Yun Liu designed and performed the experiments, analyzed the date and wrote the paper; Yanjun Guan and Kai Zhang analyzed the data and provided the helpful discussion.

Conflicts of Interest: The authors declare no conflict of interest.

Abbreviations

The following abbreviations are used in this manuscript:

AAEMs	alkali and alkali earth metals
TGA	thermo-gravimetric analyzer
VRM	volumetric reaction model

DAEM	distributed activation energy model
FMA	free-model approach
E_A	Activation energy
SEM	scanning electron microscopy
EDS	energy dispersive X-ray spectroscopy

References

1. Wang, S.J.; Fang, C.L.; Guan, X.L.; Pang, B.; Ma, H.T. Urbanization, energy consumption, and CO_2 emissions in China: a panel data analysis of China's province. *Appl. Energy* **2014**, *136*, 738-749.
2. Zhao, B.T.; Tao, W.W.; Zhong, M.; Su, Y.X.; Cui, G.M. Process, performance and modeling of CO_2 capture by chemical -absorption using high gravity: A review. *Renew. Sust. Energ. Rev.* **2016**, *65*, 44-56.
3. Muhammad, F.I.; Muhammad, U.; Kusakabe, K. Coal gasification in CO_2 atmosphere and its kinetics since 1948: a brief review. *Energy* **2011**, *36*, 12-40.
4. Xiong, J.; Zhou, Z.J.; Xu, S.Q.; Yu, G.S. Effect of alkali metal on rate of coal pyrolysis and gasification. *CIESC Journal* **2011**, *62*, 192-198. (In Chinese)
5. Joanne, T.; Sankar, B. Kinetics of CO_2 and steam gasification of Victorian brown coal chars. *Chem. Eng. J.* **2016**, *285*, 331-340.
6. Li, J.B.; Zhu, M.M.; Zhang, Z.Z.; Zhang, K.; Shen, G.Q.; Zhang, D.K. The mineralogy, morphology and sintering characteristics of ash deposits on a probe at different temperatures during combustion of blends of Zhundong lignite and a bituminous coal in a drop tube furnace. *Fuel Process. Technol.* **2016**, *149*, 176-186.
7. Tang, J.; Wang, J. Catalytic steam gasification of coal char with alkali carbonates: A study on their synergic effects with calcium hydroxide. *Fuel Process. Technol.* **2016**, *142*, 34-41.
8. Meng, L.L.; Wang, M.J.; Yang, H.M.; Ying, H.Y.; Chang, L.P. Catalytic effect of alkali carbonates on CO_2 gasification of Pingshuo coal. *Mining Science and Technology* **2011**, *21*, 587-590. (In Chinese)
9. Marc, B.; Kaveh, N.; Michael, M. Release of alkali metal, sulphur and chlorine species during high-temperature gasification and co-gasification of hard coal, refinery residue, and petroleum coke. *Fuel* **2014**, *126*, 62-68.
10. Dimple, M. Q.; Wu, H.W.; Li, C.Z. Volatilisation and catalytic effects of alkali and alkaline earth metallic species during the pyrolysis and gasification of Victorian brown coal. Part Ⅰ. Volatilisation of Na and Cl from a set of NaCl-loaded samples. *Fuel* **2002**, *81*, 143-149.
11. Wu, H.W.; Dimple, M.Q.; Li, C.Z. Volatilisation and catalytic effects of alkali and alkaline earth metallic species during the pyrolysis and gasification of Victorian brow coal. Part Ⅲ. The importance of the interactions between volatiles and char at high temperature. *Fuel* **2002**, *81*, 1033-1039.
12. Ding, L. Z.; Zhou, J.; Guo, Q.H. Catalytic effects of Na_2CO_3 additive on coal pyrolysis and gasification. *Fuel* **2015**, *142*, 134-144.
13. Walker, P.L.; Matsumoto, S.; Hanzawa, T. Catalysis of gasification of coal-derived cokes and chars. *Fuel* **1983**, *62*, 140-149.
14. Bai, Y.H.; Zhu, S.H.; Luo, K.; Gao, M.Q.; Yan, L.J.; Li, F. Coal char gasification in H_2O/CO_2: Release of alkali and alkaline earth metallic species and their effects on reactivity. *Appl. Therm. Eng*. **2017**, *112*, 156-163.
15. Kosminski, A.; Ross, D.P.; Agnew, J.B. Transformations of sodium during gasification of low-rank

coal. *Fuel Process. Technol*. **2006**, *87*, 93-952.

16. Kosminski, A.; Ross, D.P.; Agnew, J.B. Reactions between sodium and silica during gasification of a low-rank coal. *Fuel Process. Technol.* **2006**, *87,* 1037-1049.
17. Kosminski, A.; Ross, D.P.; Agnew, J.B. Reactions between sodium and kaolin during gasification of a low-rank coal. *Fuel Process. Technol.* **2006**, *87*, 1051-1062.
18. Huo, W.; Zhou, Z.J.; Wang, F.C.; Yu, G.S. Mechanism analysis and experimental verification of pore diffusion on coke and coal char gasification with CO_2. *Chem. Eng. J*. **2014**, *244*, 227-233.
19. Silbermann, R.; Gomez, A.; Gates, I.; Mahinpey, N. Kinetic studies of a novel CO_2 gasification method using coal from deep unmineable seams. *Ind. Eng. Chem. Res*. **2013**, *52*, 14787-14797.
20. Kouichi, M.; Taisuke, M. A simple method for estimating f (E) and k_0 (E) in the distributed activation energy model. *Energ. Fuel.* **1998**, *12*, 864-869.
21. Nader, M.; Arturo, G. Review of gasification fundamentals and new findings: Reactors, feedstock, and kinetic studies. *Chem. Eng. Sci*. **2016**, *148*, 14-31.
22. Arturo, G.; Nader, M. A new method to calculate kinetic parameters independent of the kinetic model: insights on CO_2 and steam gasification. *Chem. Eng. Res. Des*. **2015**, *95*, 346-357.
23. Arturo, G.; Nader, M. Kinetic study of coal steam and CO_2 gasification: A new method to reduce interparticle diffusion. *Fuel* **2015**, *148*, 160-167.
24. Gomez, A.; Silbermann, R.; Mahinpey, N. A comprehensive experimental procedure for CO_2 coal gasification: Is there really a maximum reaction rate? *Appl. Energy* **2014**, *124*, 73-81.
25. Skodras, G.; Nenes, G.; Zafeiriou, N. Low rank coal-CO_2 gasification: Experimental study, analysis of the kinetic parameters by Weibull distribution and compensation effect. *Appl. Therm. Eng*. **2015**, *74*, 111-118.
26. Micco, G.D.; Nasjleti, A.; Bohe, A.E. Kinetics of the gasification of a Rio Turbio coal under different pyrolysis temperatures. *Fuel* **2012**, *95*, 537-43.
27. Yang, Y.M.; Wu, Y.X.; Zhang, H.; Zhang, M.; Liu, Q.; Yang, H.R.; Lu, J.F. Improved sequential extraction method for determination of alkali and alkaline earth metals in Zhundong coals. *Fuel* **2016**, *181*, 951-957.
28. Tae, W.K.; Jung, R.K.; Sang, D.K.; Won, H.P. Catalytic steam gasification of lignite char. *Fuel* **1988**, *6*, 416.